

**Revised version 1134R**

**New structural data reveal benleonardite to be a member of the pearceite-polybasite group**

LUCA BINDI<sup>1,\*</sup>, CHRISTOPHER J. STANLEY<sup>2</sup>, PAUL G. SPRY<sup>3</sup>

<sup>1</sup>*Dipartimento di Scienze della Terra, Università di Firenze, Via G. La Pira 4, I-50121 Firenze, Italy*

<sup>2</sup>*Natural History Museum, Cromwell Road, London SW7 5BD, United Kingdom*

<sup>3</sup>*Department of Geological and Atmospheric Sciences, 253 Science I, Iowa State University, Ames, Iowa 50011-3210, U.S.A.*

\* e-mail address: [luca.bindi@unifi.it](mailto:luca.bindi@unifi.it)

**ABSTRACT**

The determination of the crystal structure of benleonardite (S.G.  $P\bar{3}m1$ ;  $R = 0.0321$  for 1250 reflections and 102 parameters; refined formula  $\text{Ag}_{15.0}\text{Cu}_{1.0}\text{Sb}_{1.58}\text{As}_{0.42}\text{S}_{7.03}\text{Te}_{3.97}$ ) obtained using data from a gem-quality, untwinned crystal recovered from the type material, revealed that benleonardite exhibits the structure observed for minerals of the pearceite-polybasite group. The structure consists in the stacking of  $[\text{Ag}_6(\text{Sb,As})_2\text{S}_6\text{Te}]^{2-}$  *A* and  $[\text{Ag}_9\text{Cu}(\text{S,Te})_2\text{Te}_2]^{2+}$  *B* layer modules in which (Sb,As) forms isolated  $\text{SbS}_3$  pyramids typically occurring in sulfosalts, Cu links two (S,Te) atoms in a linear coordination, and Ag occupies sites with coordination ranging from quasi linear to almost triangular. The silver  $d^{10}$  ions are found in the *B* layer module along two-dimensional diffusion paths and their electron densities, which are evidenced by means of a combination of a Gram-Charlier development of the atomic displacement factors and a split model. In the structure, two S-positions are completely replaced by Te (i.e., Te3 and Te4) and one for one half [S1:  $\text{S}_{0.514(9)}\text{Te}_{0.486}$ ],

26 whereas S2 is completely filled by sulfur. This distribution reflects on the crystal-chemical  
27 environments of the different cations. On the basis of information gained from this  
28 characterization, the crystal-chemical formula of benleonardite was revised according to the  
29 structural results, yielding  $\text{Ag}_{15}\text{Cu}(\text{Sb,As})_2\text{S}_7\text{Te}_4$  ( $Z = 1$ ) instead of  $\text{Ag}_8(\text{Sb,As})\text{Te}_2\text{S}_3$  ( $Z = 2$ )  
30 as previously reported. Thus, the mineral must be considered a member of the pearceite-  
31 polybasite group. A recalculation of the chemical data listed in the scientific literature for  
32 benleonardite according to the structural results obtained here leads to an excellent agreement.

33

34 **Keywords:** benleonardite, crystal structure, pearceite, polybasite, Ag-sulfosalt, Bambolla.

35

## 36 INTRODUCTION

37 Benleonardite, ideally  $\text{Ag}_8(\text{Sb,As})\text{Te}_2\text{S}_3$ , was identified as a new mineral species by  
38 Stanley *et al.* (1986) by studying ore minerals collected from the spoil tips of the abandoned  
39 Bambolla mine, Moctezuma, Sonora (Mexico). It was described as forming thin black  
40 powdery crusts (1–2 mm thick) with native silver, acanthite, hessite, cervelleite, pyrite and  
41 sphalerite. By means of powder-diffraction X-ray investigations, benleonardite was originally  
42 given as tetragonal with  $a = 6.603(5)$  and  $c = 12.726(6)$  Å, but the crystal structure remained  
43 unknown. Although benleonardite-like minerals have been found in several occurrences  
44 [Zyranov gold deposit, Russia (Aksenov *et al.*, 1969), Ivigtut cryolite deposit, Greenland  
45 (Karup-Møller and Pauly, 1979), Gies gold–silver telluride deposit, Montana (Zhang and  
46 Spry, 1994; Spry and Thieben, 1996), Mayflower gold–silver telluride deposit, Montana  
47 (Spry and Thieben, 1996), Um Samiuki Zn–Pb–Cu–Ag volcanogenic massive sulfide deposit,  
48 Egypt (Helmy *et al.*, 1999; Pals and Spry, 2003), black smoker chimney fragments from the  
49 Yaman Kasy massive sulfide deposit, southern Urals (Herrington *et al.*, 1998)], no additional  
50 structural investigations have been reported in the literature so far.

51 The simplified formula for benleonardite was given as  $\text{Ag}_8\text{SbTe}_2\text{S}_3$  by Stanley *et al.*,  
52 (1986). However, such a chemical formula is unbalanced, which is a very unusual  
53 characteristic when dealing with Ag-sulfosalts (Bindi and Evain, 2007; Mořlo *et al.*, 2008).  
54 Moreover, chemical data reported for benleonardite (and benleonardite-like minerals) in the  
55 literature show a general deficiency in Ag+Cu (i.e., <8 atoms per formula unit) coupled with  
56 an excess in S (i.e., 3 to 4 atoms per formula unit) when normalized on the basis of 14 atoms,  
57 thus reinforcing the suggestion by Spry and Thieben (1996) that the formula proposed by  
58 Stanley *et al.* (1986) needs to be modified.

59 Here we present the determination of the crystal structure of benleonardite obtained  
60 using data from a gem-quality, untwinned benleonardite crystal recovered from the type  
61 material. We show that benleonardite exhibits the structure observed for the minerals of the  
62 pearceite-polybasite group (Bindi *et al.*, 2006a, 2006b, 2007a, 2007b, 2007c, 2013; Bindi and  
63 Menchetti, 2009; Evain *et al.*, 2006a, 2006b).

64  
65  
66

## THE HOLOTYPE

67 A crystal for the X-ray investigation was selected from the type material (catalogue  
68 number E.1161 BM 1985, 354). The specimen was collected by the late Alan Criddle on a  
69 field excursion to the Sonora Desert led by the late Sid Williams. It consists of black powdery  
70 crusts (1–2 mm thick) of benleonardite, acanthite, hessite and cervelleite together with gangue  
71 quartz and dolomite (Fig. 1). The hessite contains a vermiform or myrmekitic intergrowth of  
72 fine-grained cervelleite (pale-greenish-grey in Fig. 1). The assemblage occupies irregular  
73 fractures in a highly altered rock described by Williams (1982) as an intensely silicified  
74 rhyolitic vitrophyre.

75  
76

77 **X-RAY CRYSTALLOGRAPHY**

78 A benleonardite crystal was hand-picked from a polished section of the type material,  
79 glued to a glass rod and used for the room temperature data collection, which was carried out  
80 on a Oxford Diffraction Xcalibur 3 diffractometer, fitted with a Sapphire 2 CCD detector (see  
81 Table 1 for details) using graphite-monochromatized MoK $\alpha$  radiation ( $\lambda = 0.71069$  Å).  
82 Because of the typical ionic conductivity observed in Ag-sulfosalts and the probable presence  
83 of twinning (see Bindi *et al.*, 2006a), a rather high  $\sin(\theta)/\lambda$  cutoff and a full sphere exploration  
84 were considered. Intensity integration and standard Lorentz-polarization correction were  
85 performed with the *CrysAlis* RED (Oxford Diffraction, 2006) software package. The program  
86 ABSPACK in *CrysAlis* RED (Oxford Diffraction, 2006) was used for the absorption  
87 correction.

88 The unit-cell found for the selected benleonardite crystal is trigonal (hexagonal setting),  
89 with  $a = 7.623(1)$  and  $c = 12.708(1)$  Å. The  $c$ -parameter is almost the same as that found by  
90 Stanley *et al.* (1986), 12.726(6) Å, and the  $a$ -parameter is related to that originally reported  
91 [i.e., 6.606(5) Å] by a factor of  $\sin(120^\circ)$  [i.e.,  $7.623$  Å  $\times$   $\sin(120^\circ) = 6.602$  Å], which  
92 explains the symmetry change from the trigonal to the tetragonal setting. The refined trigonal  
93 unit-cell obtained for benleonardite is very similar to that observed for minerals belonging to  
94 the pearceite-polybasite group (Bindi *et al.*, 2007a). Taking into account this similarity, the  
95 structure was refined in the space group  $P\bar{3}m1$  using the program JANA2006 (Petříček *et al.*,  
96 2006) starting from the atomic coordinates given by Bindi *et al.* (2007b) for the crystal  
97 structure of polybasite-*Tac*. The sites with partial (or total) substitution of S by Te were easily  
98 identified (i.e., S1, S3 and S4). To mimic the silver electron spreading along diffusion paths,  
99 up to third-order non-harmonic Gram-Charlier tensors were used for the Debye-Waller  
100 description of the Ag3, Ag4 and Ag5 atoms (Johnson and Levy, 1974; Kuhs, 1984).

101 Full site occupation (Sb/As and S1/Te1) was assured through constraints and the overall  
 102 charge balance was ascertained. The final residual  $R$  is 0.0179 for 609 reflections [ $I > 2\sigma(I)$ ]  
 103 and  $R = 0.0321$  for all 1250 unique reflections and 102 parameters.

104 Atomic parameters are reported in Tables 2 to 4, whereas bond distances are given in  
 105 Table 5. Structure factors and CIF are deposited with the Principal Editor of Mineralogical  
 106 Magazine at [http://www.minersoc.org/pages/e\\_journals/dep\\_mat.html](http://www.minersoc.org/pages/e_journals/dep_mat.html).

107 Unfortunately, the crystal used for the structural study was lost in an attempt to embed  
 108 it in epoxy to get electron microprobe data. However, the final refined formula can be written  
 109 as:  $\text{Ag}_{15.00}\text{Cu}_{1.00}(\text{Sb}_{1.58}\text{As}_{0.42})\text{S}_{7.03}\text{Te}_{3.97}$ , which is in good agreement with those reported by  
 110 Stanley *et al.* (1986) for benleonardite from the type material, i.e.  $\text{Ag}_{16.0-16.1}\text{Cu}_{0.0-0.1}\text{Sb}_{1.6-}$   
 111  $_{1.7}\text{As}_{0.4-0.6}\text{S}_{6.7-6.8}\text{Te}_{3.9-4.0}$ .

112

### 113 DESCRIPTION OF THE STRUCTURE

114 On the whole, the benleonardite structure resembles that of the trigonal polytype (*Tac*)  
 115 of polybasite (Bindi *et al.*, 2007b). It can be described as the succession, along the  $c$  axis, of  
 116 two layer modules: a  $[\text{Ag}_6(\text{Sb,As})_2\text{S}_6\text{Te}]^{2-}$   $A$  module layer and a  $[\text{Ag}_9\text{Cu}(\text{S,Te})_2\text{Te}_2]^{2+}$   $B$   
 117 module layer (Fig. 2).

118 In the  $A$  module layer, Ag atoms (Ag1 and Ag2) are triangularly coordinated by S and  
 119 Te atoms in a quasi-planar environment. Benleonardite represents the first member of the  
 120 pearceite-polybasite group showing structural disorder also in the Ag positions of the  $A$  layer.  
 121 The disorder has been modeled with two split Ag-positions ( $\text{Ag1}-\text{Ag2} = 0.51 \text{ \AA}$ ) with partial  
 122 occupancy (Table 2). The (Sb,As) atoms are also in a threefold coordination, but in a trigonal  
 123 pyramidal configuration. The  $[\text{Ag}(\text{S,Te})_3]$  and  $[(\text{Sb,As})\text{S}_3]$  subunits are linked together  
 124 through corners to constitute the  $A$  module layer.

125 In the *B* module layer, the silver  $d^{10}$  cations are distributed along 2D diffusion paths, in  
126 a structure skeleton made of face-sharing tetrahedra (as in argyrodite-type ionic-conductor  
127 compounds; Boucher *et al.*, 1993) around the Cu atom (see Fig. 3). It is worth noting that the  
128 modes (maxima of density) observed in the diffusion paths do not correspond to the Ag  
129 refined positions (Ag3, Ag4 and Ag5) and that and the refined atomic positions do not lie  
130 along diffusion paths between modes, the Gram-Charlier expansion of the Debye-Waller  
131 factor providing the connecting density. For this reason, the refined Ag positions should not  
132 be used to calculate distances (although meaningful distances could be obtained with mode  
133 positions).

134 In the structure, two S-positions are completely replaced by Te (i.e., Te3 and Te4) and  
135 one for one half [S1:  $S_{0.514(9)}Te_{0.486}$ ], whereas S2 is completely filled by sulfur. This  
136 distribution reflects on the crystal-chemical environments of the different cations. The Cu-  
137 S1/Te1 distance [2.317(4) Å] is much longer than both the Cu-S1/Se1' distance in  
138 selenopolybasite [2.199(2) Å – Evain *et al.*, 2006b] and that observed for Te-rich polybasite  
139 [2.201(2) Å; Bindi *et al.*, 2013], with an ‘S1’ occupation of  $S_{0.91(1)}Te_{0.09}$ . Although strongly  
140 enhanced (given the high amount of tellurium present in benleonardite), most of the metal-  
141 anion bond distances for the crystal studied here show a similar tendency to those in both Te-  
142 rich polybasite (Bindi *et al.*, 2013) and selenopolybasite (Evain *et al.*, 2006b).

143 Table 6 compares the X-ray powder pattern reported by Stanley *et al.* (1986) with that  
144 calculated using the structural parameters obtained in this study. Calculated and observed data  
145 are in very good agreement.

146

## 147 NOMENCLATURE REMARKS

148 The crystal structure of benleonardite is topologically identical to all compounds of the  
149 pearceite/polybasite group in their higher temperature form [i.e., 111 pearceite-type structure

150 (*Tac* polytype); Bindi *et al.*, 2007a]. The real difference is the presence of pure (Te<sub>3</sub> and Te<sub>4</sub>)  
151 and partial (S<sub>1</sub>/Te<sub>1</sub>) Te-sites. Evain *et al.* (2006b) and Bindi *et al.* (2007d, 2013) already  
152 noted that these anion sites are the same where the S-for-(Se,Te) substitution occurs in  
153 selenopolybasite and Te-rich polybasite. However, the concentration of Te in benleonardite is  
154 much higher, almost dominating three structural sites. Bindi *et al.* (2013) suggested the  
155 possible existence of a “*telluropolybasite*” in nature. In this context, benleonardite clearly  
156 represents the missing “*telluropolybasite*” member of the pearceite-polybasite group. A  
157 recalculation of the chemical data listed in the scientific literature (Table 7) for benleonardite  
158 (and benleonardite-like minerals), according to the structural results obtained here, leads to an  
159 excellent agreement. Indeed, the mean values for the sums (Ag+Cu), (Sb+As) and (Te+S) in  
160 atoms per formula unit (when the data are normalized on the basis of 29 atoms) are 16.11(13),  
161 1.98(19) and 10.91(22), in good accord with the (Ag,Cu)<sub>16</sub>(Sb,As)<sub>2</sub>(S,Te)<sub>11</sub> stoichiometry of  
162 the pearceite-polybasite minerals.

163         It is interesting to note that very high amounts of Te and Se substituting for S are always  
164 associated with low Cu contents and with disordered trigonal structures (*Tac* polytype). Such  
165 a feature was already observed and discussed by Evain *et al.* (2006b) and Bindi *et al.* (2013).  
166 Benleonardite exhibits this even more strongly, given the fact that some of the analyses given  
167 in Table 7 (corresponding to benleonardite and benleonardite-like minerals) show no  
168 appreciable concentrations of Cu. This fact seems to contradict what is known for pearceite-  
169 polybasite minerals, wherein copper is an essential element for the linearly-coordinated  
170 structural site of the *B* module layer. The case of benleonardite shows that the linearly  
171 coordinated structural site is able to accommodate larger amounts of silver than recognized  
172 previously, thus corroborating the suggestions of Bindi and Menchetti (2009) and raising the  
173 possibility that a mineral with Ag > Cu at this site deserves its own name.

174

175 **Acknowledgements**

176 The paper benefited by the official reviews made by Peter Leverett and two anonymous  
177 reviewers. Associate Editor Andrew G. Christy is thanked for his efficient handling of the  
178 manuscript. This work was supported by “Progetto d’Ateneo 2013, University of Firenze” to  
179 LB.

180

181

182 **REFERENCES**

183 Aksenov, V.S., Gavrilina, K.S., Litvinovich, A.N., Bespaev, K.H.A., Pronin, A.P., Kosyak,  
184 E.A. and Slyasarev, A.P. (1969) Occurrence of new minerals of silver and tellurium in  
185 ores of the Zyranov deposits in the Altai (in Russian). *Altai Izvestiya Akademiyi Nauk*  
186 *Kazakh SSR, Seriya Geologicheskaya*, **3**, 74–78.

187 Bindi, L. and Evain, M. (2007) Gram-Charlier development of the atomic displacement  
188 factors into mineral structures: The case of samsonite,  $\text{Ag}_4\text{MnSb}_2\text{S}_6$ . *American*  
189 *Mineralogist*, **92**, 886–891.

190 Bindi, L., Evain, M. and Menchetti, S. (2006a) Temperature dependence of the silver  
191 distribution in the crystal structure of natural pearceite,  $(\text{Ag,Cu})_{16}(\text{As,Sb})_2\text{S}_{11}$ . *Acta*  
192 *Crystallographica*, **B62**, 212–219.

193 Bindi, L., Evain, M. and Menchetti, S. (2007b) Complex twinning, polytypism and disorder  
194 phenomena in the crystal structures of antimonpearceite and arsenopolybasite. *Canadian*  
195 *Mineralogist*, **45**, 321–333.

196 Bindi, L., Evain, M. and Menchetti, S. (2007d) Selenopolybasite,  
197  $[(\text{Ag,Cu})_6(\text{Sb,As})_2(\text{S,Se})_7][\text{Ag}_9\text{Cu}(\text{S,Se})_2\text{Se}_2]$ , a new member of the pearceite-polybasite  
198 group from the De Lamar Mine, Owyhee county, Idaho, USA. *Canadian Mineralogist*,  
199 **45**, 1525–1528.



- 200 Bindi, L., Evain, M., Pradel, A., Albert, S., Ribes, M. and Menchetti, S. (2006b) Fast ionic  
201 conduction character and ionic phase-transitions in disordered crystals: The complex  
202 case of the minerals of the pearceite-polybasite group. *Physics and Chemistry of*  
203 *Minerals*, **33**, 677–690.
- 204 Bindi, L., Evain, M., Spry, P.G. and Menchetti, S. (2007a) The pearceite-polybasite group of  
205 minerals: Crystal chemistry and new nomenclature rules. *American Mineralogist*, **92**,  
206 918–925.
- 207 Bindi, L., Evain, M., Spry, P.G., Tait, K.T. and Menchetti, S. (2007c) Structural role of  
208 copper in the minerals of the pearceite-polybasite group: The case of the new minerals  
209 cupropearceite and cupropolybasite. *Mineralogical Magazine*, **71**, 641–650.
- 210 Bindi, L. and Menchetti, S. (2009) Adding further complexity to the polybasite structure: The  
211 role of silver in the *B* layer of the *M2a2b2c* polytype. *American Mineralogist*, **94**, 151–  
212 155.
- 213 Bindi, L., Voudouris, P. and Spry, P.G. (2013) Structural role of tellurium in the minerals of  
214 the pearceite-polybasite group. *Mineralogical Magazine*, **77**, 419–428.
- 215 Boucher, F., Evain, M. and Brec, R. (1993) Distribution and ionic diffusion path of silver in  $\gamma$ -  
216  $\text{Ag}_8\text{GeTe}_6$ : A temperature dependent anharmonic single crystal structure study. *Journal*  
217 *of Solid State Chemistry*, **107**, 332–346.
- 218 Downs, R.T., Bartelmehs, K.L., Gibbs, G.V. and Boisen, M.B.Jr. (1993) Interactive software  
219 for calculating and displaying X-ray or neutron powder diffractometer patterns of  
220 crystalline materials. *American Mineralogist*, **78**, 1104–1107.
- 221 Evain, M., Bindi, L. and Menchetti, S. (2006a) Structural complexity in minerals: twinning,  
222 polytypism and disorder in the crystal structure of polybasite,  $(\text{Ag,Cu})_{16}(\text{Sb,As})_2\text{S}_{11}$ .  
223 *Acta Crystallographica*, **B62**, 447–456.

- 224 Evain, M., Bindi, L. and Menchetti, S. (2006b) Structure and phase transition in the Se-rich  
225 variety of antimonpearceite,  $(\text{Ag}_{14.67}\text{Cu}_{1.20}\text{Bi}_{0.01}\text{Pb}_{0.01}\text{Zn}_{0.01}\text{Fe}_{0.03})_{15.93}(\text{Sb}_{1.86}\text{As}_{0.19})_{2.05}$   
226  $(\text{S}_{8.47}\text{Se}_{2.55})_{11.02}$ . *Acta Crystallographica*, **B62**, 768–774.
- 227 Helmy, H.M., Kamel, O.A. and El Mahallawi, M.M. (1999) Silver and silver-bearing  
228 minerals from the Precambrian volcanogenic massive sulfide deposit, Um Samiuki,  
229 Eastern Desert, Egypt. In: Stanley *et al.* (eds) *Mineral deposits: processes to processing*.  
230 Balkema, Rotterdam, pp 163–166.
- 231 Herrington, R.J., Maslennikov, V.V., Stanley, C.J. and Buslaev, F. (1998) Tellurium-bearing  
232 phases in black smoker chimney fragments from the Silurian Yaman Kasy massive  
233 sulphide orebody, southern Urals, Russia. *17<sup>th</sup> General Meeting International*  
234 *Mineralogical Association*, Toronto, Abst Prog, A119 (Abstract).
- 235 Johnson, C.K. and Levy, H.A. (1974) *International Tables for X-ray Crystallography*, edited  
236 by J. A. Ibers and W. C. Hamilton, Vol. IV, pp. 311-336. Birmingham: Kynoch Press.
- 237 Karup-Møller, S. and Pauly, S. (1979) Galena and associated ore minerals from the cryolite at  
238 Ivigtut, S. Greenland. *Meddelelser om Grønland Geoscience*, **2**, 1–25.
- 239 Kuhs, W.F. (1984) Site-symmetry restrictions on thermal-motion-tensor coefficients up to  
240 rank 8. *Acta Crystallographica*, **A40**, 133–137.
- 241 Moëlo, Y., Makovicky, E., Mozgova, N.N., Jambor, J.L., Cook, N., Pring, A., Paar, W.H.,  
242 Nickel, E.H., Graeser, S., Karup-Møller, S., Balić Žunić, T., Mumme, W.G., Vurro, F.,  
243 Topa, D., Bindi, L., Bente, K. and Shimizu, M. (2008) Sulfosalt systematics: a review.  
244 Report of the sulfosalt sub-committee of the IMA Commission on Ore Mineralogy.  
245 *European Journal of Mineralogy*, **20**, 7–46.
- 246 Oxford Diffraction (2006) *CrysAlis RED* (Version 1.171.31.2) and *ABSPACK* in *CrysAlis*  
247 *RED*. Oxford Diffraction Ltd, Abingdon, Oxfordshire, England.

- 248 Pals, D.W. and Spry, P.G. (2003) Telluride mineralogy of the low-sulfidation epithermal  
249 Emperor gold deposit, Vatukoula, Fiji. *Mineralogy and Petrology*, **79**, 285–307.
- 250 Petříček, V., Dušek, M. and Palatinus, L. (2006). *JANA2006, a crystallographic computing*  
251 *system*. Institute of Physics, Academy of Sciences of the Czech Republic, Prague, Czech  
252 Republic.
- 253 Spry, P.G. and Thieben, S.E. (1996) Two new occurrences of benleonardite, a rare silver–  
254 tellurium sulphosalt, and a possible new occurrence of cervelleite. *Mineralogical*  
255 *Magazine*, **60**, 871–876
- 256 Stanley, C.J., Criddle, A.J. and Chisholm, J.E. (1986) Benleonardite, a new mineral from the  
257 Bambolla mine, Moctezuma, Sonora, Mexico. *Mineralogical Magazine*, **50**, 681–  
258 686.
- 259 Williams, S.A. (1982) Cuzticite and eztlite, two new tellurium minerals from Moctezuma,  
260 Mexico. *Mineralogical Magazine*, **46**, 257–259.
- 261 Zhang, X. and Spry, P.G. (1994) Petrological, mineralogical, fluid inclusion, and stable  
262 isotope studies of the Gies gold–silver telluride deposit, Judith Mountains, Montana.  
263 *Economic Geology*, **89**, 602–627.
- 264
- 265
- 266
- 267
- 268
- 269
- 270
- 271

272 **FIGURE CAPTIONS**

273 Figure 1 – Reflected plane polarized light digital image in oil immersion illustrating a band of  
274 benleonardite on a ragged quartz grain to the right with rosettes of acanthite  
275 intergrown with low reflecting unidentified phases in a mass of creamy white to off-  
276 white hessite. The hessite contains a vermiform or myrmekitic intergrowth of fine-  
277 grained cervelleite (pale-greenish-grey). The sample (catalogue number E.1161 BM  
278 1985, 354) is the type specimen for both benleonardite and cervelleite.

279 Figure 2 – Projection of the benleonardite structure along the  $a$  axis. The figure emphasizes  
280 the succession of the  $[\text{Ag}_6(\text{Sb,As})_2\text{S}_6\text{Te}]^{2-}$   $A$  and  $[\text{Ag}_9\text{Cu}(\text{S,Te})_2\text{Te}_2]^{2+}$   $B$  module  
281 layers. Grey, light blue, yellow, orange and red circles refer to Ag, Cu, S (S2), S/Te  
282 (S1) and Te (Te3 and Te4), respectively.

283 Figure 3 – Non-harmonic joint probability density isosurface of silver for benleonardite at  
284 room temperature. S/Te and Cu atoms have an arbitrary size. Level of the 3D map:  
285  $0.05 \text{ \AA}^{-3}$ . The figure illustrates the silver diffusion in the  $ab$  plane among the various  
286 S/Te tetrahedral sites.

TABLE 1. Details pertaining to the single-crystal X-ray data collection and structure refinement of benleonardite

<i>Crystal data</i>	
space group	$P\bar{3}m1$ (#164)
cell parameters	$a = 7.623(1)$ (Å) $c = 12.708(1)$ (Å) $V = 639.5(2)$ (Å <sup>3</sup> )
$Z$	1
crystal color	black
crystal shape	block
crystal size (mm)	$0.031 \times 0.045 \times 0.062$
<i>Data collection</i>	
diffractometer	Oxford Diffraction Xcalibur 3
radiation type	MoK $\alpha$ ( $\lambda = 0.71073$ )
monochromator	oriented graphite (002)
scan mode	$\phi/\omega$
temperature (K)	293
detector to sample distance (cm)	5
number of frames	598
rotation width per frame (°)	0.15
measuring time (s)	90
maximum covered $2\theta$ (°)	$75.52$ ( $d = 0.86$ Å)
range of $h, k, l$	$-11 \leq h \leq 11, -13 \leq k \leq 13, -20 \leq l \leq 20$
collected reflections	11025
$R_{\text{int}}$ before absorption correction	0.1054
$R_{\text{int}}$ after absorption correction	0.0355
<i>Refinement</i>	
refinement coefficient	$F^2$
No. of refl. in refinement	1250
No. of observed refl.	609
No. of refined parameters	102
weighting scheme	$w = 1 / [\sigma^2(I) + (0.044 \times I)^2]$
$R^\dagger$ (obs) / $R^\dagger$ (all)	0.0179 / 0.0321
$wR^{2\dagger}$ (obs) / $wR^{2\dagger}$ (all)	0.0167 / 0.0172
diff. Fourier (e <sup>-</sup> /Å <sup>3</sup> )	[-1.94, 1.13]

Note:  $\dagger R = \sum ||F_o| - |F_c|| / \sum |F_o|$ .  $wR^2 = [\sum w (|F_o|^2 - |F_c|^2)^2 / \sum w (|F_o|^4)]^{1/2}$ .

TABLE 2. Wyckoff positions, site occupation factors, fractional atomic coordinates, and equivalent isotropic displacement parameters ( $\text{\AA}^2$ ) for the selected benleonardite crystal.

atom	Wyckoff	s.o.f.	$x$	$y$	$z$	$U_{\text{iso}}$
Sb	$2d$	0.789(4)	0.3333	0.6667	0.38572(2)	0.0251(7)
As	$2d$	0.211	0.3333	0.6667	0.38572(2)	0.0251(7)
Ag1	$6i$	0.677(7)	0.2848(3)	0.1424(3)	0.3804(1)	0.0526(3)
Ag2	$6i$	0.311(7)	0.3422(3)	0.1711(3)	0.3537(3)	0.0700(8)
Ag3	$12j$	0.307(5)	0.252(3)	0.3641(4)	0.1192(3)	0.0555(8)
Ag4	$12j$	0.134(6)	0.382(3)	0.402(3)	0.1065(8)	0.0635(6)
Ag5	$12j$	0.315(7)	0.3503(4)	0.2803(18)	0.1234(4)	0.0670(6)
Cu	$1a$	1.000	0	0	0	0.0320(2)
S1	$2c$	0.514(9)	0	0	0.1823(2)	0.0271(9)
Te1	$2c$	0.486	0	0	0.1823(2)	0.0271(9)
S2	$6i$	1.000	0.01458(5)	0.50729(5)	0.30681(8)	0.0404(2)
Te3	$2d$	1.000	0.6667	0.3333	0.01650(3)	0.0475(1)
Te4	$1b$	1.000	0	0	0.5	0.0422(1)

TABLE 3 – Anisotropic displacement parameters  $U_{ij}$  ( $\text{\AA}^2$ ) for the selected benleonardite crystal

atom	$U^{11}$	$U^{22}$	$U^{33}$	$U^{12}$	$U^{13}$	$U^{23}$
Sb	0.0235(9)	0.0235(9)	0.037(1)	0.0118(5)	0	0
As	0.0235(9)	0.0235(9)	0.037(1)	0.0118(5)	0	0
Ag1	0.0542(5)	0.0502(2)	0.0547(6)	0.0271(3)	-0.0002(3)	-0.0001(1)
Ag2	0.093(1)	0.0447(5)	0.089(1)	0.0464(6)	0.042(2)	0.0208(8)
Ag3	0.26(2)	0.0381(7)	0.0516(9)	-0.016(3)	-0.035(3)	0.0024(4)
Ag4	0.169(7)	0.240(9)	0.085(4)	0.170(8)	0.073(5)	0.078(6)
Ag5	0.0356(8)	0.29(1)	0.050(1)	-0.016(2)	0.0068(5)	-0.009(2)
Cu	0.0388(2)	0.0388(2)	0.0186(3)	0.0194(1)	0	0
S1	0.038(3)	0.038(3)	0.006(2)	0.019(1)	0	0
Te1	0.038(3)	0.038(3)	0.006(2)	0.019(1)	0	0
S2	0.0227(3)	0.0418(3)	0.0503(4)	0.0113(1)	-0.0031(2)	-0.0015(1)
Te3	0.0454(1)	0.0454(1)	0.0519(2)	0.02269(7)	0	0
Te4	0.0424(2)	0.0424(2)	0.0417(3)	0.02120(8)	0	0

TABLE 4. Higher-order displacement parameters<sup>†</sup> for the selected benleonardite crystal

	Ag3	Ag4	Ag5
$C^{111}$	-0.01(4)	0.08(3)	0.001(1)
$C^{112}$	0.001(9)	0.08(3)	-0.002(2)
$C^{113}$	-0.008(5)	0.028(7)	-0.0001(4)
$C^{122}$	0.000(3)	0.09(4)	0.02(1)
$C^{123}$	0.002(1)	0.028(8)	-0.0005(7)
$C^{133}$	0.0009(9)	0.006(2)	-0.0001(2)
$C^{222}$	-0.001(1)	0.11(4)	-0.06(5)
$C^{223}$	0.0002(3)	0.028(9)	0.005(3)
$C^{233}$	-0.0005(2)	0.005(3)	-0.0006(6)
$C^{333}$	-0.0001(2)	0.001(1)	0.0007(2)

Note: <sup>†</sup>Third-order tensor elements  $C^{ijk}$  are multiplied by  $10^3$ ;



TABLE 5. Main interatomic distances (Å) for the selected benleonardite crystal

Sb/As - S2	2.331(1) (×3)	Cu - S1/Te1	2.317(4) (×2)	Ag1 - S2	2.591(2) (×2)
<Sb/As-S>	2.331	<Cu-S/Te>	2.317	- Te4	2.418(2)
				<Ag1-S/Te>	2.533
Ag2 - S2	2.302(4) (×2)	Ag3 <sup>‡</sup> - S1/Te1	2.589(6)	Ag4 <sup>‡</sup> - Te3	2.726(3)
- Te4	2.926(4)	- Te3	2.692(6)	- Te3	2.720(2)
<Ag2-S/Te>	2.510	<Ag3-S/Te>	2.638	<Ag4-Te>	2.723
Ag5 <sup>‡</sup> - S1/Te1	2.559(5)				
- Te3	2.618(6)				
<Ag5-S/Te>	2.589				

Note: <sup>‡</sup> the bond distances calculated for Ag3, Ag4 and Ag5 correspond to the most probable distance calculated from the modes (maxima) of *jpdf* (joint probability density function) maps.

TABLE 6. X-ray powder diffraction patterns for benleonardite.

1			2		
<i>hkl</i>	<i>d<sub>calc</sub></i> (Å)	<i>I<sub>calc</sub></i>	<i>hkl</i>	<i>d<sub>obs</sub></i> (Å)	<i>I/I<sub>o</sub></i>
001	12.7080	79	001	12.7	70
100	6.6017	33	010	6.62	15
002	6.3540	10	002	6.34	15
101, 011	5.8584	20	011	5.87	15
102, 012	4.5780	2	012	4.61	15
003	4.2360	2	—	—	—
110	3.8115	1	—	—	—
013, 103	3.5652	23	—	—	—
200	3.3009	1	—	—	—
112	3.2685	28	—	—	—
021, 201	3.1948	31	021, 004	3.188	30
004	3.1770	56	022	2.936	100
022, 202	2.9292	100	014	2.863	25
014	2.8628	2	—	—	—
113	2.8334	5	023	2.608	35
023	2.6037	21	005	2.542	10
005	2.5416	1	—	—	—
210	2.4952	3	n.i.	2.453	15
211	2.4485	5	—	—	—
114	2.4404	54	015	2.376	15
105	2.3719	1	220	2.328	20
122, 212	2.3225	2	221, 024	2.291	10
024, 204	2.2890	26	030	2.206	10
300	2.2006	22	124	2.158	35
031, 301	2.1683	23	006	2.120	20
123, 213	2.1499	31	130, 032	2.084	10
006	2.1180	1	016	2.020	15
115	2.1146	29	n.i.	1.965	10
032, 302	2.0794	11	—	—	—
106	2.0168	4	n.i.	1.914	15
205	2.0138	19	—	—	—
214	1.9623	1	—	—	—
033	1.9528	7	007	1.819	15
220	1.9058	43	026	1.786	10
221	1.8847	3	—	—	—
116	1.8514	8	—	—	—
310	1.8310	1	134	1.744	15
222	1.8254	1	—	—	—
026, 206	1.7826	14	—	—	—
125, 215	1.7806	4	—	—	—
017	1.7504	4	—	—	—
223	1.7380	12	—	—	—
313, 133	1.6807	6	—	—	—
401	1.6367	2	—	—	—
224	1.6343	2	—	—	—
216	1.6147	4	—	—	—

042, 402	1.5974	10			
027, 207	1.5907	3	008	1.591	15
008	1.5885	9			
403	1.5378	3			
306	1.5260	2	n.i.	1.531	15
225	1.5247	5			
320	1.5145	1	—	—	—
321	1.5039	4	—	—	—
404, 044	1.4646	6	—	—	—
410	1.4406	3	—	—	—
028, 208	1.4314	6	—	—	—
226	1.4167	5	—	—	—
142, 412	1.4050	5	—	—	—
037	1.4004	2	—	—	—
045	1.3842	3	—	—	—
019	1.3808	2	—	—	—
119	1.3241	2	—	—	—
414, 144	1.3120	4	—	—	—
046	1.3018	3	—	—	—
325	1.3011	2	—	—	—
317	1.2892	2	—	—	—
038, 308	1.2880	4	—	—	—
0010	1.2708	1	—	—	—
330	1.2705	1	—	—	—
145, 415	1.2533	3	—	—	—
332	1.2458	1	—	—	—
421	1.2416	1	—	—	—
422, 242	1.2242	6	—	—	—
228	1.2202	3	—	—	—
054	1.2192	1	—	—	—
243	1.1968	3	—	—	—
146	1.1912	2	—	—	—
0210	1.1859	4	—	—	—
237	1.1630	4	—	—	—
048	1.1445	2	—	—	—
153, 513	1.1418	3	—	—	—
335	1.1364	3	—	—	—
056	1.1205	1	—	—	—
425	1.1200	4	—	—	—
319	1.1181	1	—	—	—
0310	1.1005	1	—	—	—
600	1.1003	3	—	—	—
426	1.0750	3	—	—	—
155	1.0745	1	—	—	—
063	1.0649	1	—	—	—
2210	1.0573	1	—	—	—
520	1.0571	1	—	—	—
239	1.0328	2	—	—	—
247	1.0282	1	—	—	—
1112	1.0203	2	—	—	—
0212	1.0084	2	—	—	—

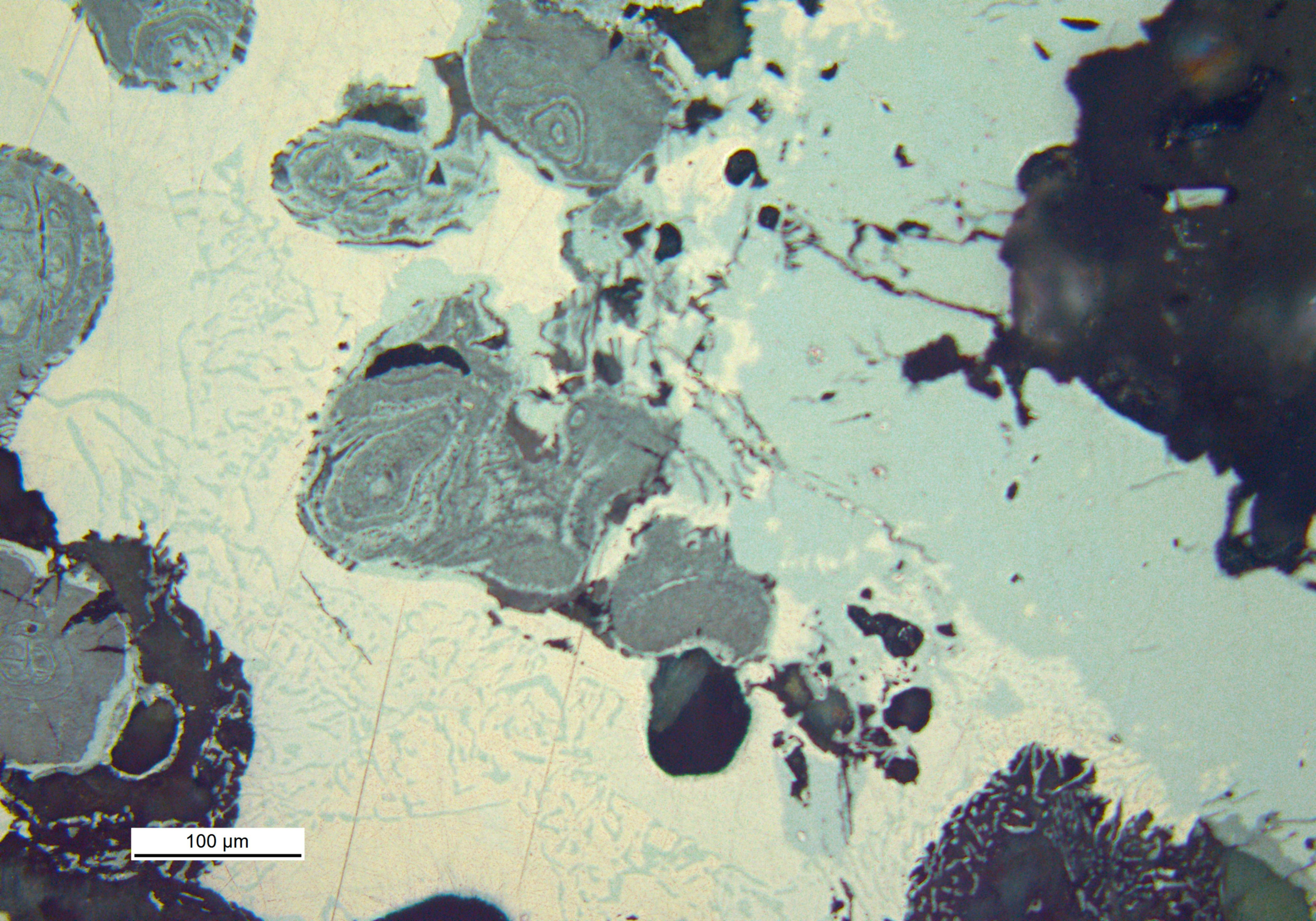
4010	1.0069	2			-		-		-
------	--------	---	--	--	---	--	---	--	---

*Note:* 1 = calculated powder pattern and indexing for benleonardite of this study. *d* values calculated on the basis of  $a = 7.623(1) \text{ \AA}$ ,  $c = 12.708(1) \text{ \AA}$ , and with the atomic coordinates and occupancies reported in Table 2. Intensities calculated using XPOW software version 2.0 (Downs *et al.*, 1993). 2 = observed powder pattern and indexing originally reported by Stanley *et al.* (1986).

TABLE 7 – Electron microprobe data (wt% of elements) of ‘benleonardite’ minerals from different deposits (data from literature) and atomic ratios calculated on the basis of 29 atoms.

	<i>Bambolla</i>						<i>Gies</i>			
	<b>1</b>	<b>2</b>	<b>3</b>	<b>4</b>	<b>5</b>	<b>6</b>	<b>7</b>	<b>8</b>	<b>9</b>	<b>10</b>
Ag	63.80	65.00	65.00	65.10	65.60	64.50	62.52	62.99	62.70	63.40
Cu	0.10	0.00	0.00	0.00	0.00	0.10	1.90	1.65	1.90	2.10
Sb	9.00	7.40	7.80	7.60	7.20	7.30	6.25	5.33	6.70	4.40
As	0.70	1.80	1.20	1.10	1.80	1.40	1.16	1.70	0.90	2.60
Te	18.60	18.40	18.70	18.50	18.70	18.70	19.38	19.06	19.60	18.80
S	8.00	8.10	8.20	8.10	8.00	8.00	8.16	8.33	8.40	8.60
total	100.20	100.70	100.90	100.40	101.30	100.00	99.37	99.06	100.20	99.90
Ag	16.01	16.11	16.10	16.23	16.22	16.14	15.52	15.60	15.41	15.38
Cu	0.04	0.00	0.00	0.00	0.00	0.04	0.80	0.69	0.79	0.87
Sb	2.00	1.63	1.71	1.68	1.58	1.62	1.37	1.17	1.46	0.95
As	0.25	0.64	0.43	0.39	0.64	0.50	0.41	0.61	0.32	0.91
Te	3.95	3.86	3.92	3.90	3.91	3.96	4.07	3.99	4.07	3.86
S	6.75	6.76	6.84	6.80	6.65	6.74	6.83	6.94	6.95	7.03
Ag+Cu	16.05	16.11	16.10	16.23	16.22	16.18	16.32	16.29	16.20	16.25
Sb+As	2.25	2.27	2.14	2.07	2.22	2.12	1.78	1.78	1.78	1.86
Te+S	10.70	10.62	10.76	10.70	10.56	10.70	10.90	10.93	11.02	10.89
	<i>Mayflower</i>		<i>Iviglut</i>	<i>Emperor</i>	<i>Um Samiuki</i>					
	<b>11</b>	<b>12</b>	<b>13</b>	<b>14</b>	<b>15</b>	<b>16</b>	<b>17</b>			
Ag	60.76	63.07	61.70	63.00	64.87	65.50	64.83			
Cu	2.68	0.55	0.00	0.18	0.30	0.00	0.31			
Sb	6.94	6.98	7.10	5.81	6.60	6.99	6.88			
As	1.15	1.01	0.00	1.57	1.71	1.20	1.66			
Te	18.97	18.75	17.00	19.99	19.24	18.78	19.98			
S	8.78	8.56	8.80	8.22	8.47	8.27	8.38			
total	99.28	98.92	94.60	98.77	101.19	100.74	102.04			
Ag	14.85	15.74	15.98	15.85	15.88	16.22	15.81			
Cu	1.11	0.23	0.00	0.08	0.12	0.00	0.13			
Sb	1.50	1.54	1.63	1.30	1.43	1.53	1.48			
As	0.40	0.36	0.00	0.57	0.60	0.43	0.58			
Te	3.92	3.95	3.72	4.25	3.98	3.93	4.12			
S	7.22	7.18	7.67	6.95	6.99	6.89	6.88			
Ag+Cu	15.96	15.97	15.98	15.93	16.00	16.22	15.94			
Sb+As	1.90	1.90	1.63	1.87	2.03	1.96	2.06			
Te+S	11.14	11.13	11.39	11.20	10.97	10.82	11.00			

Note: analyses 1-6: Stanley *et al.* (1986); analyses 7-8: Spry and Thieben (1996); analyses 9-10: Zhang and Spry (1994); analysis 11-12: Spry and Thieben (1996); analysis 13: Karup-Møller and Pauly (1979); analysis 14: Pals and Spry (2003); analysis 15-17: Pals and Spry (2003).



100 μm

